

Optical and Magnetic Properties of Copper Doped Zinc Oxide Nanofilms

Shifeng Zhao*, Yulong Bai, Jieyu Chen, Alima Bai, and Wei Gao

School of Physical Science and Technology, Inner Mongolia University, Hohhot, 010021, People's Republic of China
Inner Mongolia Key Lab of Nanoscience and Nanotechnology, Inner Mongolia University, Hohhot, 010021, People's Republic of China

(Received 26 January 2014, Received in final form 13 March 2014, Accepted 13 March 2014)

Copper doped Zinc Oxide nanofilms were prepared using a simple and low cost wet chemical method. The microstructures, phase structure, Raman shift and optical absorption spectrum as well as magnetization were investigated for the nanofilms. Room temperature ferromagnetism has been observed for the nanofilms. Structural analyses indicated that the films possess wurtzite structure and there are no segregated clusters of impurity phase appreciating. The results show that the ferromagnetism in Copper doped Zinc Oxide nanofilms is driven either by a carrier or defect-mediated mechanism. The present work provides an evidence for the origin of ferromagnetism on Copper doped Zinc Oxide nanofilms.

Keywords : magnetic properties, optical properties, ZnO, nanofilms

1. Introduction

Diluted magnetic semiconductors (DMSs) are having drawn a continually increasing interest in the past few years due to their important roles in spintronics [1, 2]. The development of practical semiconductor spintronics devices will require the development of new DMSs with Curie temperature well above room temperature (RT). Theoretical development has shown that transition metal (TM) doped wide band-gap semiconductors such as Zinc Oxide (ZnO) are the most promising candidate for achieving high Curie temperature ferromagnetism [3-6]. This has been supported by ab initio calculations based on the local density approximation (LDA) on ferromagnetic (FM) semiconductors [7, 8]. A great researches on (TM) doped ZnO and RT FM have been reported [9-19], which makes them a promising candidate material for the next generation of spintronic devices utilizing electronically optically controlled magnetism. However, experimental observations of ferromagnetism DMSs still remain controversial. Some researches believed that different magnetic response reported for ZnO-based DMSs are due to inclusions of foreign phases of various transition metal oxides [9-13]. However, others have proposed that donors and acceptors play important roles in the magnetic origin for ZnO-based

DMSs [14-19]. In order to eliminate the debate of the magnetic-metal clustering, a non-ferromagnetic metal is a good choice as a doped metal. It is known that metallic Cu and its clusters or compounds (Cu_2O and CuO) are no-ferromagnetic. Ye *et al.* indicated that in Cu-doped ZnO whether n type or p type the energy of the ferromagnetic state is lower than that of the antiferromagnetic state [20], thus room temperature ferromagnetism is expected to achieve for Cu-doped ZnO films. Recently investigations on Cu doped ZnO films have drawn increasing interests because metallic copper and its oxides (Cu_2O , CuO) are no-ferromagnetic in nature, which increases the chances of DMS which has ferromagnetism only due to doping. Cu doped ZnO films have been obtained by pulse laser ablation, magnetron sputtering [21-23] and so on. Thus, in this work, Cu doped ZnO nanofilms were prepared by a simple and low cost wet chemical method, and the optical and magnetic properties for Cu doped ZnO nanofilms were investigated in detail.

2. Experiments

The pure and Cu doped ZnO nanostructured films were prepared by solution-gelation process and spin-coating technique. The solution preparation is improved based on the work of D. R. Gamelin [24, 25]. A 0.552 M $[\text{N}(\text{Me})_4\text{OH}]$ in ethanol was added dropwise at approximately 2 mL/min to a solution of 0.101 M $\text{Zn}(\text{OAc})_2 \cdot 2\text{H}_2\text{O}$ in dimethyl sulfoxide (DMSO) under constant stirring, and the volume

©The Korean Magnetism Society. All rights reserved.

*Corresponding author: Tel: +86-471-499-3141

Fax: +86-471-499-3141, e-mail: zhsf@imu.edu.cn

ratio of them is 1:3. Different concentrations of Cu doping was achieved by addition of $\text{Cu}(\text{OAc})_2 \cdot \text{H}_2\text{O}$ to $\text{Zn}(\text{OAc})_2$ solution. The concentration of Cu doping is set to 8%, Cu doped ZnO nanoparticles were precipitated from DMSO by addition of 1-docanamine, washed with ethanol. The final solution is formed by dispersing the nanoparticles into methylbenzene. These final solutions were spin coated onto the Pt/Ti/SiO₂/Si substrate and quartz glass to form nanostructured films. The films were annealed at 400 °C in a rapid annealing oven for 5 minutes under the oxygen atmosphere with O₂ flow of 2 L/min.

The morphology examinations for the films were carried out by scanning electron microscopy (SEM, LEO-1530VP). The phase structures of the samples were characterized by x-ray diffraction (XRD) on a D/MAX-RA diffractometer using $\text{CuK}\alpha$ radiation. Optical measurements (absorption) were acquired with a UV-visible spectrophotometer. The Raman spectra were recorded on a confocal Raman spectroscope (NT-MDT NTEGRA Spectra) using a 473 nm excitation laser with an initial power of 10 mW. The field dependent magnetizations for the films were measured by using the superconducting quantum interference device (SQUID) magnetometer.

3. Results and Discussion

Figure 1(a) and (b) present the SEM image and the XRD patterns of the typical pure ZnO films and Cu doped ZnO films. Figure 1(a) shows that the film is very compact and well-structured. To confirm the elemental composition in the films, an energy dispersive x-ray (EDX) microanalysis connected to SEM was further performed. The EDX results confirmed that the molar ratio of Cu:Zn for the nanoparticles was approximately 0.04:0.96. As shown in Figure 1(b), except for the substrate signals, all the observed diffraction peaks of pure ZnO nanofilms and

Cu doped ZnO nanofilms can be indexed to a wurtzite structure as ZnO, and no any secondary or impurity phases are observed. The absence of the diffraction peaks of CuO and Cu phase structures in the XRD patterns implies Cu incorporation with the ZnO by the means of substitution for Zn. Besides, it is worth noting that, compared to the pure ZnO nanofilms, the intensity of the wurtzite diffraction peaks appreciably decreases for Cu doped ZnO nanofilms, which could be ascribed to the deformation of wurtzite lattice due to Cu doping.

The UV-visible absorption spectra of the pure and Cu doped ZnO nanofilms are investigated at room temperature. As shown in Figure 2, we can find that the optical absorption spectra changes after doping Cu from the spectra. For the pure and doping ZnO films, the absorption coefficient α and optical band-gap E_g obey the following relation $\alpha^2 = A(h\nu - E_g)$. In order to evaluating the band-gap (E_g), inset of Figure 2 presents the dependence of α^2 as a function of $h\nu(E)$ for the pure and Cu doped ZnO nanofilms. It is easy to find that the optical band-gap of the films narrows from 3.21 eV to 2.98 eV after doping

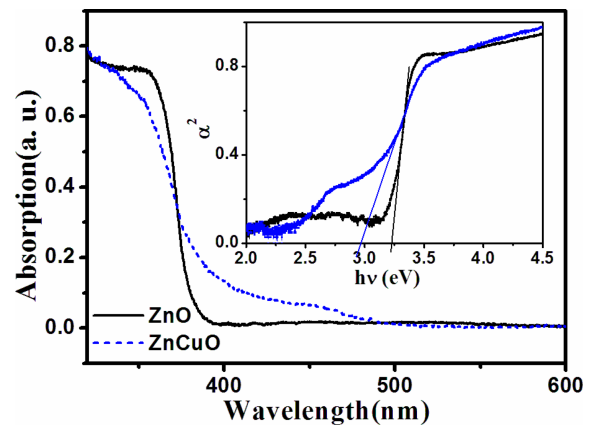


Fig. 2. (Color online) Optical absorption spectroscopy of pure and Cu doped ZnO nanofilms.

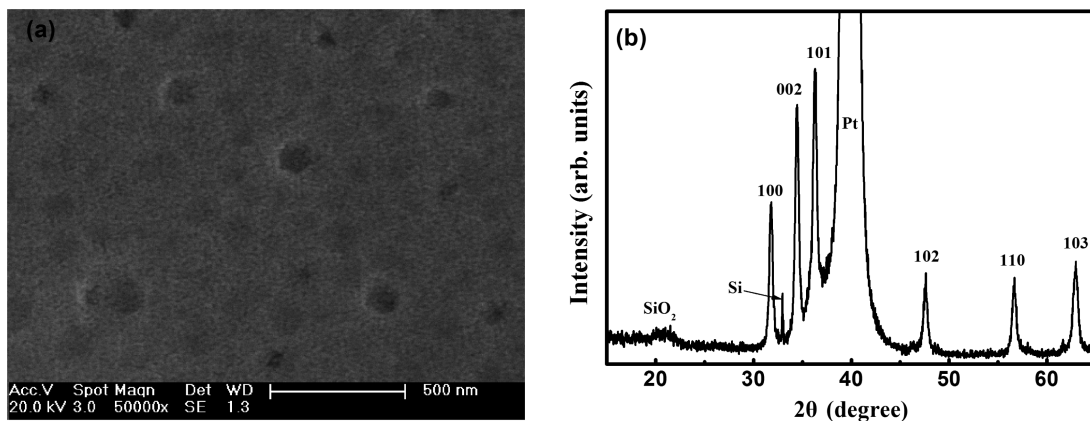


Fig. 1. (a) The SEM image of the typical Cu doped ZnO films, (b) the XRD pattern of pure and Cu doped ZnO nanofilms.

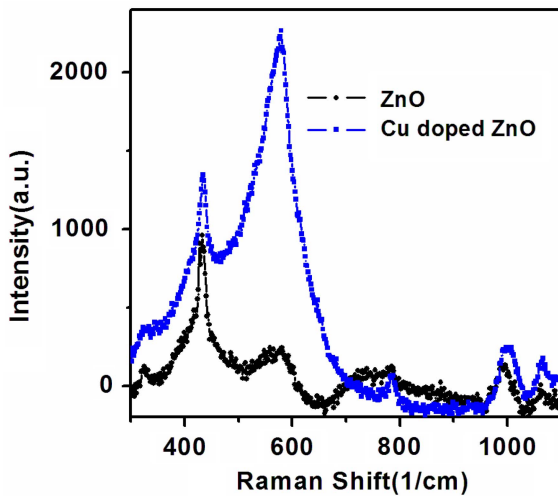


Fig. 3. (Color online) The Raman shift spectra for pure and Cu doped ZnO nanofilms.

Cu.

The decrease of the band-gap after doping Cu is probably related to the increase of lattice constant and difference in ionicity between Zn-O and Cu-O bonds. Moreover, the chemical and magnetic effects, since Zn and Cu atoms have strong mismatch in electronegativity, is also a reason for the decrease of the band-gap. In fact, with the increase of the Cu doping concentration, the band-gap of the films decrease, which is consistent with the results coming from the first-principles calculations based on density functional theory [26].

Figure 3 presents Raman scattering spectrum of Cu doped ZnO films as well as ZnO films. As can be seen, there are two very extinct peaks at 433 cm^{-1} and 577 cm^{-1} , which are the characteristic wurtzite E_2 (high) mode and A_1 longitudinal optical (LO) mode [$A_1(\text{LO})$] [27, 28]. It is worth noting that the intensity ratio of the two peaks changes very strongly after doping Cu for the ZnO films. For pure ZnO films, the Raman shift peak intensity of the E_2 (high) mode is much stronger than that of the $A_1(\text{LO})$ mode. However, for Cu doped ZnO films, the intensity of the $A_1(\text{LO})$ mode is increasingly stronger than that of E_2 (high) mode. This could be attributed to the following two factors: Firstly, the E_2 (high) mode is related to the symmetry of wurtzite hexagonal ZnO. Therefore, the intensity decrease of the Raman peak about E_2 (high) mode implies that the lattice symmetry is slightly influenced due to doping of Cu ions into the lattice. As well known, the ionic radius of Cu^{2+} is smaller than Zn^{2+} , thus, the symmetry of crystal will change when Cu ions substitute Zn ions position. Secondly, since $A_1(\text{LO})$ mode is mostly caused by the defects such as O-vacancy, Zn-interstitial defect, or these complexes [29], with the Cu doping, the

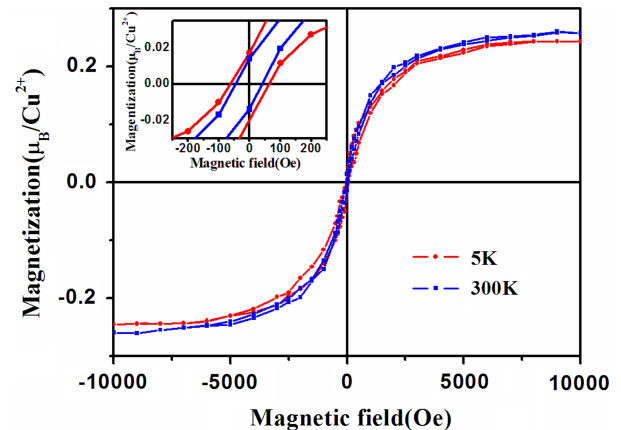


Fig. 4. (Color online) The magnetic hysteresis loops of Cu doped ZnO nanofilms.

$A_1(\text{LO})$ mode is significantly enhanced, implying the defects increasing in the crystal due to the doping of Cu. This result is coherent with the intensity decrease of any wurtzite diffraction peaks for Cu doped ZnO nanofilms as shown in Figure 1(b).

In order to reveal the magnetic behavior of the films, the magnetization dependence on the magnetic field was measured at low temperature of 5 K and room temperature of 300 K. The diamagnetic contribution from the Si substrate has been subtracted here. The magnetic hysteresis loops were plotted in Figure 4, which shows a good hysteresis shape with coercive field (H_c) of 45 Oe and 70 Oe, respectively. Thus strong room temperature ferromagnetism is observed for the films. The saturation magnetizations are about $0.24\ \mu\text{B}/\text{Cu}^{2+}$ (0.51 emu/g) and $0.26\ \mu\text{B}/\text{Cu}^{2+}$ (0.55 emu/g) at 5 K and 300 K, respectively. Thus saturation magnetization is higher than the results of previous report [30]. Besides, we note that the saturation magnetization, remanent magnetization, and coercivity at 300 K are very close to those of at 5 K. Therefore, it can be concluded that the Curie temperature of this samples are above 300 K.

For general transition metal doped ZnO films, Cu is an intrinsically nonmagnetic transition metal, and its clusters or compounds except nanocrystalline Cu_2O do not contribute to ferromagnetism. Thus, we would rather attribute the origin of the ferromagnetism to the substitution doping of the Cu iron than the contamination of ferromagnetic cluster or weak ferromagnetism induced by the transition metal oxidation of CuO. Besides, since the Raman results showed that there were large numbers of defects in Cu doped ZnO nanofilms, we suggest that more defects are also possibly responsible for the strong room-temperature ferromagnetism in the Cu doped ZnO nanofilms. Thus, the results lead us to consider that the ferromag-

netism in Cu doped ZnO nanofilms is driven either by a carrier or defect-mediated mechanism. Certainly, the effect of concentration defects or carriers on the room temperature ferromagnetism for transition metal doped ZnO films will be further carried out in the future works.

4. Conclusions

In summary, Cu-doped ZnO nanofilms were prepared by a simple wet chemical method. Optical absorption spectra indicate the band-gap of the Cu doped ZnO films is lower than that of pure ZnO films. A strong ferromagnetism is observed at room temperature. The ferromagnetism in the nanofilms was caused by a number of defects in the crystal due to the substitution of Zn^{2+} in ZnO lattice by Cu^{2+} ions, and the room-temperature ferromagnetism is an intrinsic origin rather than the contamination of ferromagnetic clusters. The present work provides an evidence for the origin of ferromagnetism on Cu doped ZnO nanofilms.

Acknowledgments

This work was financially supported by the National Natural Science Foundation of China (Grant Nos. 10904065, 11264026), the National Key Projects for Basic Research of China (2012CB626815), Program for Young Talents of Science and Technology in Universities of Inner Mongolia Autonomous Region (NJYT-12-B05), and Program of Higher-Level Talents of Inner Mongolia University (115109).

References

- [1] S. A. Wolf, D. D. Awschalom, R. A. Buhrman, J. M. Daughton, S. V. Molnár, M. L. Roukes, A. Y. Chtchelkanova, and D. M. Treger, *Science* **294**, 1488 (2001).
- [2] D. D. Awschalom and M. E. Flatté, *Nature Physics* **3**, 153 (2007).
- [3] T. Dielt, H. Ohno, F. Matsukura, J. Cibert, and D. Fermand, *Science* **287**, 1019 (2000).
- [4] J. J. Wu, S. C. Liu, and M. H. Yan: *Appl. Phys. Lett.* **85**, 1027 (2004).
- [5] Y. H. Lin, M. Ying, M. Li, X. Wang, and C. W. Nan, *Appl. Phys. Lett.* **90**, 222110 (2007).
- [6] C. L. Tsai, Y. J. Lin, J. H. Chen, H. C. Chang, Y. H. Chen, L. Horng, and Y. T. Shih, *Solid State Commun.* **152**, 488 (2012).
- [7] S. Lardjane, G. Merad, N. Fenineche, A. Billard, and H. I. Faraoun, *J. Alloys Compd.* **551**, 306 (2013).
- [8] S. P. Nanavati, V. Sundararajan, S. Mahamuni, S. V. Ghaisas, and V. Kumar, *Phys. Rev. B* **86**, 205320 (2012).
- [9] A. Wójcik, K. Kopalko, M. Godlewski, E. Guzewicz, R. Jakieła, R. Minikayev, and W. Paszkowicz, *Appl. Phys. Lett.* **89**, 051907 (2006).
- [10] N. Spaldin, *Phys. Rev. B* **69**, 125201 (2004).
- [11] T. Fukumura, Z. Jin, A. Ohmoto, H. Koinuma, and M. Kawasaki, *Appl. Phys. Lett.* **78**, 958 (2001).
- [12] M. Tay, Y. Wu, G. C. Han, T. W. Chong, Y. K. Zheng, S. J. Wang, Y. Chen, and X. Pan, *J. Appl. Phys.* **100**, 063910 (2006).
- [13] S. F. Zhao, C. H. Yao, Q. Lu, F. Q. Song, J. G. Wan, and G. H. Wang, *Transactions of Nonferrous Metals Society of China* **19**, 1450 (2009).
- [14] C. L. Tsai, Y. J. Lin, C. J. Liu, L. Horng, Y. T. Shih, M. S. Wang, C. S. Huang, C. S. Jhang, Y. H. Chen, and H. C. Chang, *Appl. Surf. Sci.* **255**, 8643 (2009).
- [15] K. R. Kittilstved and D. R. Gamelin, *J. Am. Chem. Soc.* **127**, 5292 (2005).
- [16] H. S. Hsu, J. C. A. Huang, S. F. Chen, and C. P. Liu, *Appl. Phys. Lett.* **90**, 102506 (2007).
- [17] O. Mounkachi, A. Benyoussef, A. E. Kenz, E. H. Saidi, and E. K. Hill, *J. Appl. Phys.* **106**, 093905 (2009).
- [18] B. Panigrahy, M. Aslam, and D. Bahadur, *Appl. Phys. Lett.* **98**, 183109 (2011).
- [19] C. L. Tsai, Y. J. Lin, J. H. Chen, H. C. Chang, Y. H. Chen, L. Horng, and Y. T. Shih, *Solid State Commun.* **152m**, 488 (2012).
- [20] L. H. Ye, A. J. Freeman, and B. Delley, *Phys. Rev. B* **73**, 033203 (2006).
- [21] S. Karamat, R. S. Rawat, T. L. Tan, P. Lee, S. V. Springham, Anis-ur-Rehman, R. Chen, and H. D. Sun, *J. Supercond Nov Magn.* **26**, 187 (2013).
- [22] C. Sudakar, J. S. Thakur, G. Lawes, R. Naik, and V. M. Naik, *Phys. Rev B* **75**, 054423 (2007).
- [23] D. L. Hou, X. J. Ye, H. J. Meng, H. J. Zhou, X. L. Li, C. M. Zhen, and G. D. Tang, *Appl. Phys. Lett.* **90**, 142502 (2007).
- [24] M. Purica, E. Budianu, E. Rusu, M. Danila, and R. Gavrilă, *Thin Solid Films* **403**, 485 (2002).
- [25] H. Q. Yan, R. R. He, J. Justin, L. Matthew, S. Richard, and J. P. D. Yang, *J. Am. Chem. Soc.* **125**, 4728 (2003).
- [26] M. Ferhat, A. Zaoui, and R. Ahuja, *Appl. Phys. Lett.* **94**, 142502 (2009).
- [27] A. Umar, and Y. B. Hahn, *Appl. Phys. Lett.* **88**, 173120 (2006).
- [28] J. J. Wu and S. C. Liu, *J. Phys. Chem. B* **106**, 9546 (2002).
- [29] A. K. Pradhan, K. Zhang, G. B. Loutts, U. N. Roy, Y. Cui, and A. Burger, *J. Phys. Condens. Matter* **16**, 7123 (2004).
- [30] X. F. Wang, J. B. Xu, W. Y. Cheung, J. An, and N. Ke, *Appl. Phys. Lett.* **90**, 212502 (2007).